Letters in Applied Microbiology, 2023, 76, 1–10
https://doi.org/10.1093/lambio/ovad077
Advance access publication date: 6 July 2023
Research Article

LETTERS IN APPLIED MICROBIOLOGY
OXFORD UNIVERSITY PRESS

Engineering xylose fermentation in an industrial yeast: continuous cultivation as a tool for selecting improved strains

Thalita P. Basso[1,†], Dielle P. Procópio[2,*,†], Thais H.C. Petrin[2], Thamiris G. Giacon[2], Yong-Su Jin[3,4], Thiago O. Basso[2], Luiz C. Basso[5]

[1]Department of Genetics, Escola Superior de Agricultura Luiz de Queiroz, Universidade de São Paulo, Piracicaba, SP 13418-900, Brazil
[2]Department of Chemical Engineering, Escola Politécnica, Universidade de São Paulo, São Paulo, SP 05508-010, Brazil
[3]DOE Center for Advanced Bioenergy and Bioproducts Innovation, University of Illinois at Urbana-Champaign, Urbana, IL 61801, United States
[4]Department of Food Science and Nutrition, University of Illinois at Urbana-Champaign, Urbana, IL 61801, United States
[5]Department of Biological Sciences, Escola Superior de Agricultura Luiz de Queiroz, Universidade de São Paulo, Piracicaba, SP 13418-900, Brazil

*Corresponding author. Rua do Lago, 250, Butantã, São Paulo, SP 05508-080, Brazil. E-mail: diellepierotti@gmail.com
†T.P.B. and D.P.P. contributed equally to this work.

Abstract

Production of second-generation ethanol from lignocellulosic residues should be fueling the energy matrix in the near future. Lignocellulosic biomass has received considerable attention as an alternative renewable resource toward reducing the demand for fossil energy sources, contributing to a future sustainable bio-based economy. Fermentation of lignocellulosic hydrolysates poses many scientific and technological challenges as the drawback of *Saccharomyces cerevisiae's* inability in fermenting pentose sugars (derived from hemicellulose). To overcome the inability of *S. cerevisiae* to ferment xylose and increase yeast robustness in the presence of inhibitory compound-containing media, the industrial *S. cerevisiae* strain SA-1 was engineered using CRISPR-Cas9 with the oxidoreductive xylose pathway from *Scheffersomyces stipitis* (encoded by *XYL1*, *XYL2*, and *XYL3*). The engineered strain was then cultivated in a xylose-limited chemostat under increasing dilution rates (for 64 days) to improve its xylose consumption kinetics under aerobic conditions. The evolved strain (DPY06) and its parental strain (SA-1 XR/XDH) were evaluated under microaerobic in a hemicellulosic hydrolysate-based medium. DPY06 exhibited 35% higher volumetric ethanol productivity compared to its parental strain.

Significance and impact of study

Production of biofuels from lignocellulosic biomass should be fueling the energy matrix soon. Robust yeast strains will play an important role to convert sugars from these residues, such as xylose, into fuel ethanol under industrial conditions. In this work, we engineered an industrial *S. cerevisiae* strain from sugar cane ethanol production to produce ethanol from xylose. An additional adaptive laboratory evolution (ALE) strategy was applied to further improve xylose consumption kinetics in this strain. We believe our findings could provide a basis for further studies on robust industrial strains, and it illustrates the potential of ALE for ethanol production from such residues.

Keywords: *Saccharomyces cerevisiae*, evolutionary engineering, xylose, industrial strain, chemostat cultivation

Introduction

The biomass-to-biorefinery concept is based on the replacement of first-generation feedstocks, which encompasses a great spectrum of marketable products (chemicals, materials, and food) and energy (fuels, power, and/or heat) (Cunha et al. 2020). In energy-driven biorefineries, lignocellulosic biomass is used for the production of liquid (biodiesel or bioethanol) and/or gaseous (biomethane) road transportation biofuels (Van Vleet and Jeffries 2009, Cunha et al. 2020). Lignocellulosic biomass is a potential sustainable source of various carbon sources found in several types of raw materials, ranging from urban and industrial waste, wood, and agricultural residues such as corn straw, wheat straw, rice straw, and sugar cane bagasse (Procópio et al. 2022, Qiu et al. 2023). Therefore, this material represents a partially untapped rich source for biofuels and biomaterials, constituting an important renewable alternative to petrochemicals (Van Vleet and Jeffries 2009, Cunha et al. 2020). Cost-effective bioethanol production from renewable biomass requires the efficient and complete use of all sugars present in these raw lignocellulosic materials, including all pentose and hexose sugars (Procópio et al. 2022). In particular, glucose and xylose, the major cellulose- and hemicellulose-derived sugar, respectively (Van Vleet and Jeffries 2009, Procópio et al. 2022).

With extensive use in various biotechnological applications, including first-generation biofuels, food products, biochemicals, and the pharmaceuticals industry, it was natural that *S. cerevisiae* became a microbial chassis in second-generation biofuel production (Van Vleet and Jeffries 2009, Cunha et al. 2020). Its industrial use is widespread due to its high tolerance to harsh conditions, particularly strains isolated from industrial conditions (Procópio et al. 2022). Industrial *S. cerevisiae* strains exhibit remarkable tolerance to diverse stress encountered in industrial environments, including low pH, high

Received: December 15, 2022. **Revised:** May 31, 2023. **Accepted:** July 5, 2023

osmotic pressure, elevated ethanol concentration, and phage contamination (Della-Bianca and Gombert 2013). Moreover, these strains demonstrate high ethanol productivity, attributed to the selective pressures exerted during successive fermentations and the practice of pitching between fermentation tanks (Della-Bianca and Gombert 2013, Cunha et al. 2020). These characteristics have led to the development of *S. cerevisiae* as a chassis microorganism for metabolic engineering, particularly in the valorization of lignocellulosic biomass (Cunha et al. 2020, Procópio et al. 2022). However, the use of *S. cerevisiae* for energy-driven biorefineries, requires that the xylose assimilation pathway is re-constructed in this microbial cell to overcome its inability to ferment xylose (Van Vleet and Jeffries 2009). In this regard, considerable research efforts have been dedicated to exploring the expression of various pathways involved in xylose metabolism in industrial strains of *S. cerevisiae* (Dias Lopes et al. 2017, Cunha et al. 2020). For instance, this microorganism has been engineered to express either xylose reductase-xylitol dehydrogenase (XR/XDH) genes (the so-called oxidoreductase pathway), the xylose isomerase (XI) gene, or selected genes from the nonphosphorylating portion of the Weimberg pathway (Procópio et al. 2022).

Successfully genetic engineering allows *S. cerevisiae* strains to use xylose; however, this yeast faces uptake issues for this pentose sugar, which means that improvements in efficient xylose utilization have been hampered, in part, by xylose transport capacity (Brink et al. 2021, Qiu et al. 2023). Despite this yeast has numerous monosaccharide transporters (*HXT1-17* and *GAL2*), only a few of those (*HXT1*, *HXT2*, *HXT4*, *HXT5*, *HXT7*, and *GAL2*) were identified to be able to transport xylose, albeit with a poor affinity when compared to glucose (Osiro et al. 2018). Moreover, glucose represses xylose transport by the native transporters, limiting their use in mixed sugar fermentation (Brink et al. 2021, Qiu et al. 2023). In an attempt to overcome this condition and to allow this microorganism successfully ferment the main fraction of hemicellulose (Cunha et al. 2020), some studies have focused on bioprospecting and characterizing heterologous xylose-transporters in *S. cerevisiae*, providing alternatives for efficient xylose uptake (Procópio et al. 2022, Qiu et al. 2023). Specific pentose transporters from heterologous hosts have been reviewed in detail (Qiu et al. 2023), including PsSut1, PsSut2, SsXut1, SsXut3, SsHxt2.6, and SsQup2 from *Scheffersomyces stipitis*, Cs4130 from *Candida sojae*, AnHxtB from *Aspergillus nidulans*, At5g59250/At5g17010 from *Arabidopsis thaliana*, CiGxf1 and CiGxs1 from *C. intermedia*, Mgt05196 from *Meyerozyma* (*Pichia*) *guilliermondi*, Xltr1p from *Trichoderma reesei*, and BsAraE from *Bacillus subtilis*, have been introduced into *S. cerevisiae* strains (Qiu et al. 2023). Additionally, pentose uptake limitation can be overcome by improving native transporters using a combination of bioinformatics and mutagenesis (Brink et al. 2021, Qiu et al. 2023), and by applying adaptive laboratory evolution (ALE) for the selection of advantageous mutations over time, leading to enhanced traits (Sonderegger and Sauer 2003).

The experimental situation referred to as ALE involves subjecting microorganisms to a variety of environmental stressors, such as nutrient limitations, temperature changes, or exposure to toxic compounds, with the aim of selecting for individuals with beneficial traits (Mavrommati et al. 2022). Through this process, microorganisms can accumulate mutations in their regulatory networks, some of which may improve their ability to grow or survive under imposed stressors (Mavrommati et al. 2022). Chemostats are used to obtain steady-state cultures under well-defined cultivation conditions. However, in long-term chemostat cultures, there might be accumulation of spontaneous mutations and selection under designed conditions (Sonderegger and Sauer 2003, Mavrommati et al. 2022). Although chemostat cultures for ALE require more complicated culture devices compared to colony transfer and serial transfer methods, it is less labor intensive once the operation begins (Mavrommati et al. 2022). Besides, chemostat cultivations can be used to generate high numbers of cell divisions and, thus, high number of diverse populations (Mavrommati et al. 2022). Combining rational engineering followed by ALE on xylose-containing medium under aerobic or oxygen-limited conditions has been successfully applied to generated *S. cerevisiae* strains with improved kinetics for xylose uptake (Kim et al. 2013).

Engineering *S. cerevisiae* for bioethanol production from xylose has achieved considerable progress over the last years (Dos Santos et al. 2016, Dias Lopes et al. 2017). This includes further genetic modifications, besides the introduction of xylose consumption pathway, to enhance the flux of xylose through the central carbon metabolism of the yeast, allowing for improved xylose utilization. However, the cost-efficient exploitation of hemicellulosic biomass, which is rich in xylose, depends on the development of xylose-consuming robust strains (Cunha et al. 2020, Procópio et al. 2022). Therefore, given the need for continuous development of robust microorganisms for this purpose, we performed a combination of metabolic engineering with ALE to expand the capabilities of the robust industrial *S. cerevisiae* SA-1 strain (Cola et al. 2020) for xylose utilization. SA-1 was initially engineered, using a highly efficient CRISPR-Cas9 system-based approach, with the oxidoreductase pathway from *S. stipitis* (encoded by *XYL1*, *XYL2*, and *XYL3*) (Kim et al. 2012), yielding the SA-1 XR/XDH strain. To improve xylose utilization, ALE using long-term chemostat cultivations was used to address the low xylose uptake rate of SA-1 XR/XDH. More specifically, this strain was cultured in aerobic xylose-limited chemostats, resulting in the evolved strain DPY06, which showed improved xylose fermentation performance compared to its parental strain.

Material and methods

Strains and media

The yeast strain used in this study was *S. cerevisiae* SA-1, a robust industrial strain isolated from fuel ethanol plants in Brazil (Basso et al. 2008), which was used as microbial chassis for expressing the oxidoreductase pathway for xylose consumption from *Sc. stipitis*, yielding strain SA-1 XR/XDH (Supplementary Table S1). This strain presented the genes *XYL1*, *XYL2*, and *XYL3* (Kim et al. 2012) integrated into the *URA3* locus, yielding an auxotrophic strain for uracil. Then, SA-1 XR/XDH was subjected to evolutionary engineering experiments (via adaptive laboratory evolution) in continuous cultures to improve xylose utilization, yielding strain DPY06 (Supplementary Table S1).

Strains were cultured in media composed of yeast extract and peptone (YP, 10 g L^{-1} yeast extract, 20 g L^{-1} peptone) supplemented with glucose and or/xylose at different concentrations, both in aerobic shake-flasks and anaerobic serum-bottles batch cultivations. In adaptive laboratory evolution

cultivations, strains were cultured in a defined media developed by Verduyn and co-workers (VM), as described by Verduyn et al. (1992). The medium was composed of the following components (in g L^{-1}): $(NH_4)_2SO_4$, 5.0; KH_2PO_4, 3.0; $MgSO_4.7H_2O$, 0.5; and trace-elements consisting of (in mg L^{-1}) EDTA, 15, $ZnSO_4.7H_2O$, 4.5, $MnCl_2.2H_2O$, 0.84; $CoCl_2.6H_2O$, 0.3; $CuSO_4.5H_2O$, 0.3; $Na_2MoO_4.2H_2O$, 0.4; $CaCl_2.2H_2O$, 4.5, $FeSO_4.7H_2O$, 3.0, H_3BO_3, 1.0, KI, 0.1. A solution containing vitamins was filter-sterilized and added to the medium to a final concentration of (mg L^{-1}) d-biotin, 0.05; calcium pantothenate, 1.0; nicotinic acid, 1.0; myo-inositol, 25; thiamine.HCl, 1.0; pyridoxine.HCl, 1.0, and p-aminobenzoic acid, 0.20. Uracil was added to 80 mg L^{-1}, as proposed by Basso et al. (2010) to avoid uracil limitation.

Transformation for pentose fermentation by X123 cassette insertion using CRISPR-Cas9

The three-gene cassette (P_{TDH3}-*XYL1*-T_{TDH3}, P_{PGK1}-*XYL2*-T_{PGK1}, and P_{TDH3}-*XYL3*-T_{TDH3}, referred to as X123) was integrated into the *URA3* locus using a one-step, markerless protocol mediated by CRISPR-Cas9 (Ryan et al. 2014). The plasmid pRS406-X123 expressing the three genes (*XYL1*, *XYL2*, *XYL3*) with 7692 bp in length was amplified using the primers URA_X123_foward (5′- GACTATTTGCAAAGGGAAGGGATGCTAAGGTAGA GGG TGAACGTTACAGAGAGATAGGGTTGAGTGTTGT-3′) and URA_X123_reverse (5′—CATTTACTTAT AATACAGTTTTTTAGTTTTGCTGGCCGCATCTTCTCAA AAGTTAGCTCACTCATTAGGC-3′). The reaction mixture for one PCR reaction was prepared as follows: 13 μL sterile deionized water, 21 μL of 3 M Betaine (Sigma-Aldrich), 1 μL DMSO (Sigma-Aldrich), 10 μL 5× buffer (HF), 1 μL dNTPs (10 mM each dNTP), 1 μL DNA (1-5 ng μL^{-1}), 2.5 μL of 10 μM primer mixture (forward and reverse), 0.5 μL Phusion Hot Start Flex DNA Polymerase® (New England BioLabs). PCR was performed using an Applied Biosystems VeritiTM thermal cycler with the following cycling program: initial denaturation at 98°C for 5 min; 35 cycles at 98°C for 30 seconds, 55°C for 30 seconds, 72°C for 4 min; and final extension at 72°C for 10 min. The PCR product was purified using the DNA Clean & ConcentratorTM-5 kit (ZymoResearch®).

The cassette was co-transformed into SA-1 using a Cas9 plasmid (pCas9) that expresses a sgRNA sequence includes the tRNATyr promoter, *URA3* guide, sgRNA, and SNR52 terminator. The 20 nt guide directs Cas9 to generate a double-stranded DNA break at the targeted locus (*URA3* in this case), which greatly increases the frequency of homologous recombination (Gietz and Woods 2002).

Yeast transformation was adapted from Gietz and Woods (2002). The transformation mixture was prepared in 1.5 mL tubes with 90 μL competent cells (see above), 10 μL salmon sperm DNA Life Technologies® (ssDNA) previously heated to 100°C for 5 min and kept on ice for 5 min, 1 μg pCas9, 5 μg donor DNA, 260 μL 50% polyethylene glycol (PEG 3500 w/v, Sigma-Aldrich), 36 μL 1 M LiAc. Tubes were incubated at 30°C and agitated on a tube shaker rotator for 30 min, then subjected to a heat shock (42°C for 20 min). The tubes were centrifuged at 5000 rpm for 2 min in an Eppendorf® 5424 centrifuge, the supernatant discarded and the pellets resuspended in 1 mL of YPD broth. The tubes were incubated at 30°C on a tube shaker rotator for 2 h. The tubes were centrifuged at 5000 rpm for 1 min, 700 μL of YDP removed and the pellet resuspended in the remaining volume and 300 μL was plated on YPD-A supplemented with 200 μg mL^{-1} of Geneticin® Life Technologies (G418). The plates were incubated at 30°C until isolated colonies were observed (2–4 days). After growth of isolated colonies, they were restreaked twice on YPD to lose the pCas9 plasmid. Loss of the pCas9 plasmid was confirmed by loss of G418 resistance.

Integration of the X123 cassette into the *URA3* locus was confirmed by streaking strains SA-1 and SA-1 XR/XDH, on 5-FOA plates (1 g L^{-1} of 5-FOA, 5 g L^{-1} of ammonium sulfate, 20 g L^{-1} of glucose, 20 mg L^{-1} of uracil, 1.7 g L^{-1} of yeast nitrogen base without amino acids, Difco BD). While *URA3*+ (positive) strains can metabolize 5-fluoroorotic acid (5-FOA) into a toxic compound, *URA3*− (negative) strains cannot metabolize 5-FOA and will grow normally. SA-1 XR/XDH co-transformed with the pCas9 plasmid and X123 donor DNA showed 5-FOA resistance.

In addition, correct integration was confirmed by PCR analysis and Sanger sequencing. The gDNA of SA-1 XR/XDH strain was isolated, and the URA3 regions surrounding the integration site were amplified using the following primers: X123_Up_conf_fw (5′-CCTAGTCCTGTTGCTGCCAA-3′), X123_Up_conf_rev (5′-CAGGCTGTTGTTGTCACA CG-3′), X123_Dn_conf_fw (5′- CTTTCCAACAGCCGAAACCG-3′), and X123_Dn_conf_rev (5′- GTTCCGTTTGACTTGTCGCC-3′). Purified PCR products were sequenced at Quintara Biosciences (Berkeley, CA) to confirm barcode sequence in the amplicon.

Phenotype evaluation in YPX medium

Strain without (SA-1) and with the X123 cassette (SA-1 XR/XDH) was evaluated in YPX4 medium (YP medium containing 4% xylose) using a 96-well microplate growth assay, incubated at 30°C with constant agitation (orbital shaking, frequency of 9.2 Hz; with an amplitude of 4.4 mm) under oxygen-limited condition; OD_{600} nm was measured every 15 min using Tecan Sunrise over 72 h. The 96-well microplate was set up with 130 μL of medium and 20 μL of the fresh cell suspension to have an initial OD_{600} nm of 0.3 and 150 μL final volume.

Adaptive laboratory evolution in aerobic xylose-limited chemostat cultivation

After the precultivation step of the SA-1 XR/XDH strain at 30°C and 200 rpm in 500 mL shake flasks containing 100 mL of the VM-defined medium with 20 g L^{-1} xylose and 20 mg L^{-1} uracil, yeast cells were inoculated in a 2.0 L water-jacketed model Labors 5 (Infors AG, Switzerland) bioreactor containing 0.8 L of VM defined medium, with 60 g L^{-1} xylose and 80 mg L^{-1} uracil. Bioreactor batch cultivation (BBC) was conducted until the exhaustion of xylose (which was monitored by a sharp drop in the CO_2 concentration in the off-gas analysis). After BBC, the mode of cultivation was switched to continuous through the constant addition of fresh VM medium supplemented with 20 g L^{-1} xylose and 80 mg L^{-1} uracil by a peristaltic pump. The working volume was kept constant by a mechanical drain and a peristaltic pump in line with an aseptic waste vessel. The feeding rate was adjusted during the cultivation to increase the selective pressure on cells

(please, see details in the "Results" section). Compressed air was used to flush the culture vessel (0.5 L min^{-1}). The dissolved oxygen concentration was monitored constantly by a dissolved oxygen electrode (Mettler-Toledo, Columbus, OH, USA). The agitation frequency was set to 800 rpm, the temperature was controlled at 30°C, and pH was controlled at 5.0 via a controlled 2 M KOH solution. Continuous cultivation was performed for 64 days. To isolate potential evolved strains, samples were plated from the continuous cultivation medium in a YP medium containing 20 g L^{-1} xylose (YPX2) and evaluated under aerobic (oxic) and anaerobic (anoxic) conditions (200 rpm) in shake-flask cultivations, as depicted below.

Shake-flask cultivations for strain characterization

YP medium was used for shake-flasks batch cultivations. After preinoculum, yeast cells were harvested by centrifugation at 3134 × *g*, at 4°C for 5 min, and washed three times with distilled water. Aerobic and microaerobic batch fermentation experiments were performed by inoculating the pelleted yeast cells in a 100 mL Erlenmeyer flask with 30 mL containing fermentative medium, composed of YPX (YP medium containing xylose), YPD (YP medium containing glucose), YPDX (YP medium containing glucose and xylose), or YPXH (hemicellulosic hydrolysate supplemented with 10 g yeast extract L^{-1}, 20 g peptone L^{-1}, and 40 g xylose L^{-1}). All conditions were performed at 30°C. For aerobic conditions, agitation was set at 200 rpm, while under anaerobic and microaerobic conditions, agitation was at 100 rpm. For anaerobic batch fermentation experiments, precultures were inoculated in a serum bottle containing 30 mL of fermentative medium, which could be YPX or YPDX. A serum bottle sealed with butyl rubber stoppers was used to ensure strict anaerobic (anoxic) conditions. The serum bottles with fermentation media were then flushed with nitrogen gas, previously passed through a heated, reduced copper column to remove the trace of oxygen. All cultivations were performed in biological triplicates.

The hemicellulosic hydrolysate from sugar cane straw (Brenelli et al. 2020) was kindly provided by Dra. Livia Brenelli from Centro Nacional de Pesquisa em Energia e Materiais—CNPEM, Campinas, SP, which was obtained by a two-stage procedure: mild acetylation at 60°C, 30 min, 0.8% (w/w) of NaOH and 10% (w/w) of solids followed by hydrothermal pretreatment at 190°C, 20 min, 10% (w/w) of solids. The hemicellulosic hydrolysate obtained after the second step was enzymatically treated with a GH11 from *Neocallimastix patriciarum* (Megazyme® Ireland) as detailed described elsewhere (Brenelli et al. 2020). Supplementary Table S2 shows the chemical composition of the hemicellulosic hydrolysate.

Analytical methods and physiological parameter calculations

Samples were taken at appropriate intervals to measure cell growth and metabolites. Cell growth was monitored by optical density (OD) at 600 nm using a UV-visible Spectrophotometer (BIomate 5) (Basso et al. 2010). Samples were centrifuged at 15 000 rpm for 10 min and supernatants were diluted appropriately and then used for the determination of glucose, xylose, xylitol, glycerol, succinate, acetic acid, and ethanol by high-performance liquid chromatography (Agilent Technologies 1200 Series) equipped with a refractive index detector. The Rezex ROA-Organic Acid H+ (8%) column (Phenomenex Inc., Torrance, CA) was used and the columns were eluted with 5 mM H_2SO_4 at 50°C, and the flow rate was set at 0.6 mL min^{-1}.

The maximum growth rate was obtained by plotting the natural logarithm of OD_{600} values against time and then calculating the slope of the straight line corresponding to the exponential growth phase. Yield coefficients were calculated as the absolute value of the slope of a straight line: the ethanol yield ($Y_{ethanol}$) from a plot of product concentration data against substrate concentration data (Della-Bianca and Gombert 2013).

Results and discussion

Construction of an industrial xylose-utilizing strain by integration of a three-gene cassette using CRISPR-Cas9

In this study, we measured the capacity of the industrial *S. cerevisiae* diploid strain, SA-1, to ferment xylose as a carbon source after expressing the oxidoreductase pathway for metabolizing xylose. Thereby, SA-1 was engineered for xylose utilization by integration through a CRISPR-Cas9-mediated system of a three-gene cassette (X123) that expresses three heterologous enzymes from *Sc. stipitis* necessary for xylose utilization: xylose reductase (*XYL1*), xylitol dehydrogenase (*XYL2*), and xylulokinase (*XYL3*) (Kim et al. 2012) into the *URA3* locus, yielding the SA-1 XR/XDH strain. Both SA-1 and SA-1 XR/XDH strains were evaluated in YPX4 at 30°C for 72 h, under an oxygen-limited condition in 96-well microplate equipment. Only the engineered strain, that contained the integrated xylose cassette, was able to grow in YPX under these conditions (Supplementary Fig. S1). Under this condition, the maximum growth rate (μ_{max}) of the engineered strain was 0.06 h^{-1}, which is higher than that presented by the xylose-consuming *S. cerevisiae* strain, BSN3, 0.044 h^{-1}, when cultivated under the oxygen-limited condition in YP supplemented with 4% of xylose (Li et al. 2016). In their work, Li and coauthors used the xylose-consuming diploid *S. cerevisiae* strain BSIF as the chassis cell for additional integration, including the overexpression of the genes *XKSI*, *TAL1*, *TKL1*, *RKL1*, and *RPE1* in the nonoxidative pentose phosphate pathway and the inactivation of *GRE3* and *PHO13*, yielding the strain BSIF (Li et al. 2016).

Physiological characterization of SA-1 XR/XDH at different xylose concentrations under anaerobic and microaerobic conditions

Analysis of SA-1 XR/XDH was performed in YPX medium (YP medium containing 1% xylose—YPX1, 2% xylose—YPX2, 4% xylose—YPX4, or 8% xylose—YPX8). Cells were grown under strictly anaerobic (anoxic) conditions for 624 h with an initial cell density OD_{600} of 1. The results showed that it spent >600 h to consume over 50% xylose when fermenting YPX1 (Supplementary Fig. S2a). In the same time frame, when fermenting 20 g L^{-1} xylose (YPX2), the SA-1 XR/XDH strain consumed 31% of total available sugar (Supplementary Fig. S2b), or 23% of 40 g L^{-1} xylose (YPX4) (Supplementary Fig. S2c), or 11% of 80 g L^{-1} xylose (YPX8) (Supplementary Fig. S2d). The increasing initial concentration of xylose did not improve xylose consumption by SA-1 XR/XDH.

Table 1. Physiological parameters of SA-1 XR/XDH in YPX1 (YP medium containing 10 g L^{-1} xylose), YPX2 (YP medium containing 20 g L^{-1} xylose), YPX4 (YP medium containing 40 g L^{-1} xylose), or YPX8 (YP medium containing 80 g L^{-1} xylose) under anaerobic conditions, at 30°C and 100 rpm, with initial OD_{600} of 1.

Cultivation condition	Xylose consumed (g L^{-1})	Xylose consumption rate (g L^{-1} h^{-1})	Specific xylose consumption rate (g xylose OD^{-1} h^{-1}) [OD][a]	Accumulated xylitol production (g L^{-1})	Accumulated glycerol production (g L^{-1})	Accumulated ethanol production (g L^{-1})	$Y_{Ethanol}$
YPX1	6.21 ± 0.13	0.01 ± 0.00	0.04 ± 0.01 [0.57]	1.21 ± 0.15	0.69 ± 0.15	1.6 ± 0.07	0.25 ± 0.02
YPX2	8.23 ± 0.58	0.01 ± 0.00	0.07 ± 0.02 [0.63]	1.43 ± 0.02	0.97 ± 0.03	2.34 ± 0.02	0.28 ± 0.05
YPX4	10.39 ± 1.56	0.02 ± 0.00	0.04 ± 0.01 [0.65]	1.56 ± 0.05	1.13 ± 0.09	3.22 ± 0.10	0.32 ± 0.02
YPX8	8.59 ± 1.21	0.01 ± 0.00	0.11 ± 0.07 [0.64]	1.16 ± 0.01	1.97 ± 0.27	2.14 ± 0.47	0.23 ± 0.04

[a]OD value at the maximum rate of xylose consumption. All parameters were calculated for up to 624 h of fermentation. Parameters: $Y_{Ethanol}$, Ethanol yield ($g_{ethanol}$ $g_{consumed\ xylose}^{-1}$). Data represent the average ± SD of triplicate cultivations.

The engineered strain achieved the highest ethanol concentration at 624 h of cultivation in the YPX4 medium (Table 1), which was 50%, 27%, and 34% higher for cultivation performed in YPX1, YPX2, and YPX8, respectively. Similarly, xylose metabolism rate and xylitol accumulation were higher in YPX4 cultivation. SA-1 XR/XDH (Table 1). Conversely, the highest maximum specific xylose consumption rate was observed for cultivations in YPX8 (0.11 ± 0.07 g xylose OD^{-1} h^{-1}) within the first 24 h of cultivation. Although the rate of anaerobic xylose metabolism is relatively low, when comparing anaerobic cultivation of SA-1 XR/XDH in YPX1 with an evolved laboratory strain expressing oxidoreductase pathway from *Pichia stipitis* (Sonderegger and Sauer 2003), the industrial xylose-fermenting strain described here achieved the same ethanol yield (0.25 g ethanol g consumed $xylose^{-1}$) of the 460-generation population from Sonderegger and Sauer's work.

The absence of any additional modification in SA-1 XR/XDH to address the unbalanced cofactor requirement between XR and XDH associated under anaerobic xylose fermentation resulted in the slight growth profile under strictly anaerobic (anoxic) conditions on diverse xylose concentrations (Supplementary Fig. S2). In response to the higher amount of xylose in the medium, lower xylose consumption was observed by SA-1 XR/XDH. One would think that higher xylose concentration could lead to higher xylose uptake by the yeast cell. However, this finding contradicts the expectation that higher concentrations of xylose would lead to increased uptake by yeast cells. These results suggest that catabolite repression was triggered in SA-1 XR/XDH yeast under anaerobic conditions when exposed to the highest xylose concentration tested (80 g L^{-1}). These observations are consistent with previous study of xylose-metabolizing *S. cerevisiae*, which have suggested that xylose has a depressing effect on gene expression (Salusjärvi et al. 2008).

Recent studies highlight the need to rewire global regulatory systems to address the challenge of efficiently fermenting xylose in engineered yeast. These efforts have identified several key genes targets, including *IRA2*, *ISU1*, *HOG1*, *BCY1*, *AZF1*, *GRE3*, and *MGA2*, that play a crucial role in regulating xylose metabolism. Other approaches include constructing a semisynthetic regulon based on the native galactose regulatory network, disrupting a transcription factor THI2, and overexpressing TFs *STT4*, *RGI2*, and *TFC3* (Osiro et al. 2018). Additionally, it has been demonstrated that xylose affects the SNF1/Mig1p pathway in different ways. It triggers Hxk2p autophosphorylation at Ser158, reducing its catalytic activity and glycolysis rate. SNF1 subunit Snf1p is allosterically regulated by ADP:AMP ratios but may not be affected by d-xylose due to similar energy charges (Brink et al. 2021). Additionally, *SUC2* is a gene under control of SNF1/Mig1p pathway and encodes invertase, which is repressed both on high and low glucose concentrations and induced only during low levels of glucose. A biosensor with *SUC2* driving GFP expression showed that high xylose concentrations are sensed by *S. cerevisiae* as low glucose concentrations. Both the xylose molecule and some of its intracellular metabolites are sensed by the SNF1/Mig1p pathway, as indicated by the biosensor results in nonengineered and engineered strains (Osiro et al. 2018).

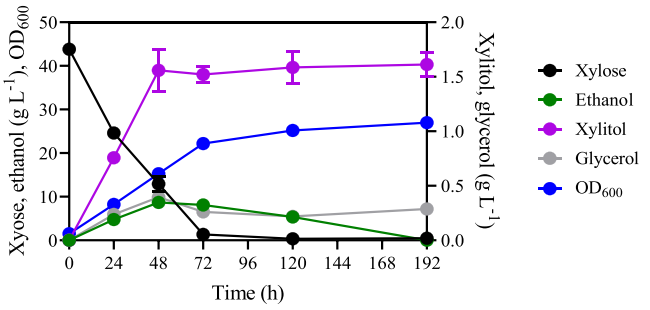

Figure 1. Microaerobic fermentation kinetics of SA-1 XR/XDH in YP medium containing 40 g L^{-1} xylose—YPX4, with initial cell density OD_{600} of 1, at 30°C and 100 rpm.

Anaerobic alcoholic fermentation of xylose without xylitol formation is possible when XR and XDH would have matching coenzyme specificities (Kuyper et al. 2004). Recent studies have demonstrated that further rational and inverse metabolic engineering strategies have improved anaerobic xylose metabolism with lesser xylitol formation of *S. cerevisiae* expressing *XYL1*, *XYL2*, and *XYL3* through concomitant deletion of *PHO13* and *ALD6*, as well as overexpression of *TAL1*, followed by laboratory adaptive evolution (Kim et al. 2012, 2013).

In contrast to the anaerobic (anoxic) condition, under microaerobic conditions, SA-1 XR/XDH could consume all xylose in 120 h of cultivation when cultivated in a YPX4 medium (Fig. 1). Xylose consumption rate dramatically increased from 0.02 ± 0.00 g L^{-1} h^{-1} to 0.36 ± 0.00 g L^{-1} h^{-1} comparing the cultivations under anaerobic and microaerobic conditions, respectively, under the same cultivation medium condition (YPX4). Within the first 72 h of cultivation, SA-1 XR/XDH consumed over 90% xylose (a total of 42.49 ± 0.82 g L^{-1}) producing 8.19 ± 0.34 g L^{-1} of ethanol (Supplementary

Table 2. Physiological parameters of SA-1 XR/XDH and DPY06 in YP media containing 20 g L^{-1} glucose and 80 g L^{-1} xylose under anaerobic conditions.

	At 24 h			At 72 h			
	r_{xylose}	r_{xylose}*	$P_{Ethanol}$	r_{xylose}	r_{xylose}*	$P_{Ethanol}$	$Y_{Ethanol}$
SA-1-XR/XDH	0.67 ± 0.07	0.14 ± 0.02	0.45 ± 0.02	0.56 ± 0.00	0.10 ± 0.00	0.24 ± 0.01	0.28 ± 0.00
DPY06	1.04 ± 0.01	0.50 ± 0.01	0.62 ± 0.01	0.79 ± 0.01	0.26 ± 0.00	0.33 ± 0.00	0.27 ± 0.00

An initial OD_{600} was adjusted to 0.3. All parameters were calculated for up 72 h of fermentation. Parameters: r_{xylose}, xylose consumption rate (g L^{-1} h^{-1}); r_{xylose}*, specific xylose consumption rate (g L^{-1} OD^{-1} h^{-1}); $P_{Ethanol}$, volumetric ethanol productivity (g L^{-1} h^{-1}); $Y_{Ethanol}$, ethanol yield (g $g_{total\ sugar}^{-1}$). Data represent the average ± SD of triplicate cultivations.

Table S3). Ethanol yield had been decreased when oxygen is available in the medium, as illustrated in Table 2 and Supplementary Table S3. Conversely, accumulated xylitol production achieved the same value for both YPX4 cultivation in anaerobic and microaerobic conditions. The presence of oxygen enables SA-1 XR/XDH to consume xylose faster; however, it was not enough to reduce xylitol production. Under similar conditions, SA-1 XR/XDH presented an increased xylose consumption profile than the YSX3 *S. cerevisiae* strain (Jeong et al. 2020). Their strain, which contains *XYL1*, *XYL2*, and *XYL3* in the chromosome, was unable to consume completely 40 g L^{-1} xylose in 100 h of cultivation.

Adaptive laboratory evolution of the industrial strain SA-1 XR/XDH in xylose-limited chemostat cultures

In order to improve the yield and/or productivity of xylose fermentation, continuous aerobically cultivation was performed in a bioreactor. Long-term adaptation experiments are an interesting approach to selecting strains with the desired phenotype (Kim et al. 2013). The ALE procedure represents one of the most practical solutions for metabolic engineering to induce spontaneous mutations, which is analogous to processes that occur in nature during the evolution of new species, favorable to heterologous metabolism (Mavrommati et al. 2022). This approach has been shown as a powerful approach for improving xylose utilization (Kim et al. 2013). Thereby, rationally designed genetic modifications combined with ALE promote generating strains able to assimilate more efficiently xylose (Mavrommati et al. 2022).

After transformant evaluation, the resulting strain SA-1 XR/XDH was grown under the stress of xylose as the sole carbon source in the VM-defined medium (Verduyn et al. 1992). The cultivation was characterized by a batch and a continuous phase. After the batch phase, denoted by the exhaustion of xylose in the bioreactor, feeding started at a fixed dilution rate. The initial flow rate was based on the maximum growth rate of the batch phase, and the flow was kept within an interval of 8–10 mL h^{-1}. Cells were cultivated at a fixed dilution rate until a decrease in xylose concentration. Therefore, as the residual xylose concentration decreased, the flow rate was augmented. Xylose consumption profile (Fig. 2a), glycerol, and xylitol production profiles (Fig. 2b) were observed during the continuous phase, but ethanol production was not.

After adaptive incubation on xylose, the cell density (measured by OD_{600}) exhibited and increase from 13.25 at 18 h to 22.8 at 63 h of cultivation. Simultaneously, the flow of fresh medium increased from 10 to 48 mL h^{-1}, corresponding to the dilution rate of 0.6 h^{-1}. The increase in the flow rate did not promote the wash-out of the cells from the bioreactor, suggesting the progress of adaptive evolution, in which less adapted cells were eliminated from these cropping, remaining evolved strains with the ability to uptake xylose faster. Among the tested isolated, the colony that grew fastest on xylose was named DPY06 (data not shown).

Physiological characterization of SA-1 XR/XDH and the evolved strain under anaerobic conditions in xylose/glucose mixtures

To check the improvements derived from the laboratory evolution approach, the evolved strain, DPY06, and its parental strain, SA-1 XR/XDH, were cultivated under strict anaerobic (anoxic) conditions in a YP medium containing 20 g L^{-1} glucose and 80 g L^{-1} xylose, at 30°C and 100 rpm in serum bottles sealed with butyl rubber stoppers with an OD_{600} of 0.3. DPY06 exhibited a different improved xylose consumption profile under anaerobic conditions in comparison with the parental strain (Fig. 3). The evolved strain consumed 71% of the initial xylose in the medium, while SA-1 XR/XDH consumed only 48% in 72 h of cultivation (Fig. 3a). For glucose metabolism, no difference was observed between the two strains. However, despite the greater consumption of xylose by the DPY06 strain, the evolved strain achieved lesser cell density than the control strain, OD_{600} of 1.22 ± 0.04 versus 5.5 ± 0.16 at 192 h of cultivation. Ethanol production was detected in both cultivations; however, DPY06 did show a slight improvement in the volumetric ethanol productivity (Table 2). The ethanol production profile was higher for DPY06 than SA-1 XR/XDH in 144 h of cultivation, 27.1 ± 0.34 against 24.4 ± 0.76 g L^{-1}, respectively (Fig. 3). At the same time, the evolved strain produced 39% more glycerol and 9% more xylitol as a by-product than the control cultivation. Moreover, despite DPY06 showing higher xylitol accumulation until 168 h of cultivation, the evolved strain exhibited lower xylitol accumulation within 192 and 240 h of fermentation than SA-1 XR/XDH.

It is interesting to note that DPY06 used the available carbon mainly to produce ethanol, xylitol, and glycerol; and minor amounts were diverted to yeast biomass in comparison to SA-1 XR/XDH, which achieved roughly the double OD_{600} reading after 24 h until the end of the cultivation. Furthermore, practically all biomass was produced during glucose depletion (first 24 h of cultivation), after that, it was no significant increments in this parameter for both strains. Xylose consumption and specific xylose consumption rates were determined and DPY06 presented high values for these parameters. Table 2 presents these values at 24 and 72 h. Therefore, under the conditions investigated, the isolated mutant has advantages in xylose fermentation.

Similar continuous cultivation under aerobic conditions was performed by Wahlbom et al. (2003) with recombi-

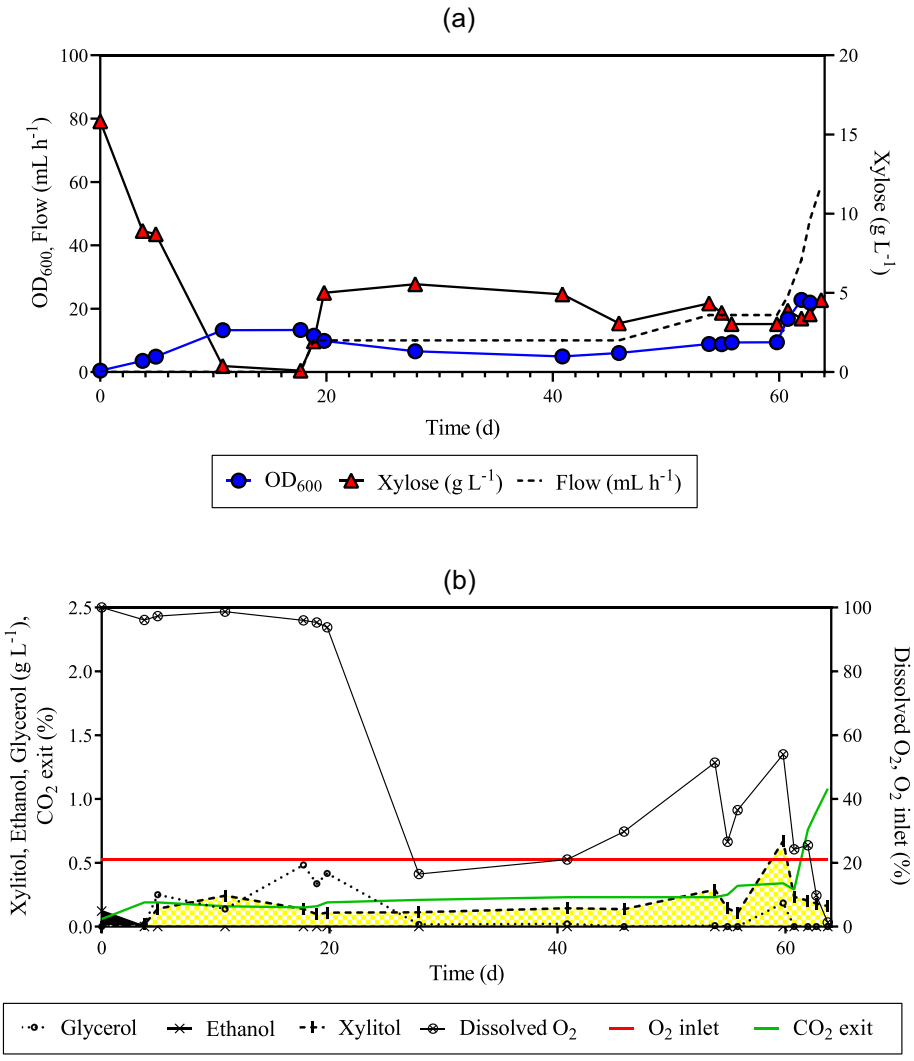

Figure 2. Long-term continuous cultivation of *S. cerevisiae* SA-1 XR/XDH under an anaerobic condition with xylose as the carbon source. (a) OD_{600} values, residual xylose concentration, and pump flow rate. (b) Glycerol, gray area; xylitol, yellow area; ethanol, black area. The batch phase lasted for 17 days.

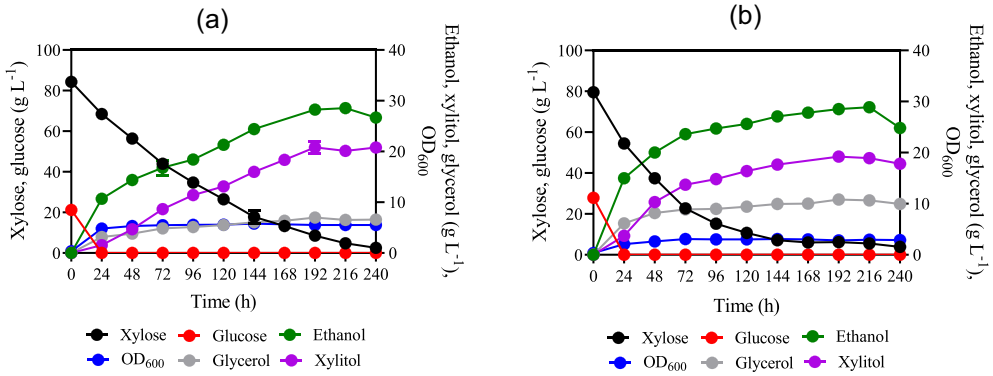

Figure 3. Anaerobic fermentation kinetics of the parental strain SA-1 XR/XDH (a) and the evolved strain DPY06 (b) in 20 g L^{-1} glucose and 80 g L^{-1} xylose in YP media. An initial OD_{600} was adjusted to 0.3. The figure illustrates the average of triplicate experiments for each strain: SA-1 XR/XDH, expressing two copies of *XYL1*, *XYL2*, and *XYL3*; and DPY06, an evolved strain from SA-1 XR/XDH.

nant xylose-utilizing *S. cerevisiae* strain TMB3399. They also performed continuous cultivation under oxygen-limited and anaerobic conditions to obtain mutants that display an improved ability to ferment xylose. However, even the best of these mutants, the strain TMB3400, showed only about one-third of the aerobic maximum growth rate obtained with *P. stipitis* CBS 6054 on xylose. Compared to its parental strain, the TMB3400 strain achieved an ethanol yield of 0.25 while

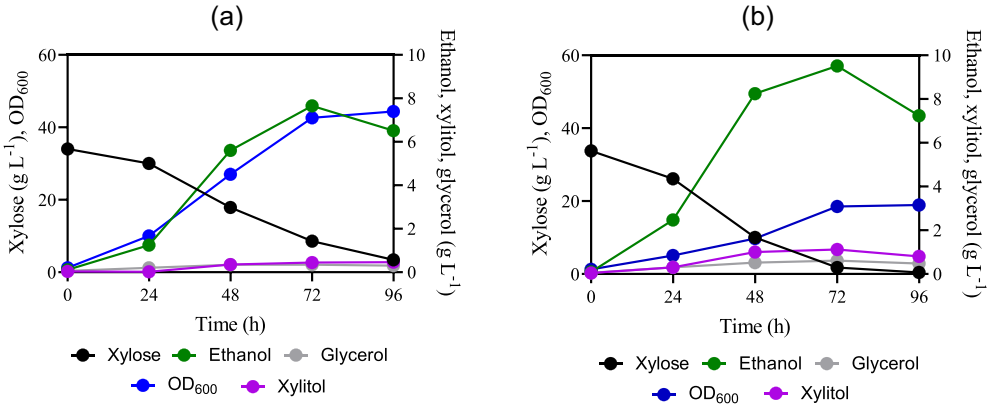

Figure 4. Representative fermentation profiles of SA-1 XR/XDH (a) and DPY06 (b) during batch cultivation in YPXH (YP medium containing hemicellulosic hydrolysate and xylose). Cultivations were performed at 30°C and 100 rpm with an initial OD_{600} of 1. Data are presented as a single replicate from three independent biological replicates.

for TMB3399, it was 0.21 g ethanol g xylose^{-1} (Wahlbom et al. 2003).

In a more recent study, Jeong et al. (2020) applied a blended approach, metabolic and evolutionary engineering, to improve xylose assimilation in a laboratory *S. cerevisiae* strain expressing XYL123, besides a deletion of *PHO13* and overexpression of *TAL1*. An adaptive evolution approach was applied, and mutants isolated from the evolved cultures showed improved xylose fermentation capabilities, with a growth rate of 0.19 g L^{-1} h^{-1} and ethanol yield of 0.32 g g^{-1} when fermenting 40 g L^{-1} of xylose in YP medium, which was higher than DPY06 strain in YPDX under microaerobic condition. In Supplementary Table S4, we benchmark some studies with xylose-utilizing strains expressed *XYL1*, *XYL2*, and *XYL3* or *XKS1* for xylose assimilation. Many studies have shown improved xylose fermentations by yeast, which suggests that multiple genetic modifications were probably necessary to endow SA-1 XR/XDH with the ability to grow faster on xylose.

Efforts also have been made to engineer industrial isolates, including diploid or polyploid strains, to enhance their ability to consume xylose. Romaní et al. (2015) reported on the successful engineering of two isolates, namely PE-2 and CAT-1, derived from the sugar cane ethanol industry, which exhibited enhanced xylose consumption capabilities. Furthermore, Cunha et al. (2019) conducted research focused on the simultaneous expression of the two metabolic pathways involved in xylose consumption in two industrial isolates. Their findings demonstrated the effectiveness of this approach. Additionally, Cunha et al. (2020) investigated the potential of employing cell-surface display of enzymes, in conjunction with the expression of the XR/XDH and XI xylose consumption pathways, in different industrial isolates. These studies highlight the ongoing progress in engineering industrial isolates to improve their xylose consumption abilities. Such advancements have significant implications for optimizing biofuel production and other industrial processes. These engineered strains offer several advantages, such as improved robustness, tolerance to toxic compounds, and suitability for large-scale bioreactor cultivation, which are essential for industrial applications (Dias Lopes et al. 2017).

These toxic compounds such as furans, organic acids, phenols, and inorganic salts are formed during lignocellulosic pretreatment (Cola et al. 2020). Since the lignocellulosic residues are attracting increasing interest worldwide as a new energy matrix, the use of robustness strains that can deal with those toxic compounds might make the industrial production of biofuels and biochemicals more profitable (Li et al. 2016, Cola et al. 2020). According to Cola et al. (2020), diploid strains, specifically SA-1, exhibit a distinct ability to grow in environments containing lignocellulosic inhibitory compounds. As presented by the authors, SA-1 demonstrated superior resistance to the individual inhibitory effects of acetic acid, levulinic acid, *p*-coumaric acid, ferulic acid, furfural, and HMF (Cola et al. 2020). Considering that the performance of recombinant strains is significantly affected by the genetic background of the host strain (Li et al. 2016), the choice of industrial diploid strains, which normally are more robust and have better ethanol producers compared to laboratory haploid strains, might represent a potential benefit for biotechnological processes (Li et al. 2016, Cola et al. 2020).

Fermentation of hemicellulosic hydrolysate

To evaluate the fermentative performance in a hemicellulosic hydrolysate, strain DPY06 and the parental strain (control) were cultivated under microaerobic conditions in a hemicellulosic hydrolysate medium supplemented with yeast extract, peptone, and xylose (YPXH), with an initial OD_{600} of 1 and 30°C (Fig. 4a and b). Under this condition, the evolved strain presented a higher ethanol concentration than the control strain (9.45 ± 0.08 versus 6.51 ± 0.05 g L^{-1} at 72 h of cultivation), which represents an increase of 31% in ethanol titers by the evolved strain in relation to the control strain. Despite the increased ethanol concentration, ethanol yield on xylose from DPY06 (0.34 ± 0.01 g ethanol g xylose^{-1}) was virtually the same as the control strain (0.35 ± 0.01 g ethanol g xylose^{-1}). In addition, the evolved strain exhibited a higher volumetric ethanol productivity throughout the cultivation period, reaching a peak at 48 h with a value of 0.17 ± 0.00 g L^{-1} h^{-1}. This represents a 35% increase compared to the volumetric ethanol productivity achieved by the SA-1 XR/XDH strain. DPY06 strain efficiently consumed nearly all xylose present in the medium within 96 h of cultivation, utilizing 33.57 ± 0.45 g of xylose, which accounted for 98.6% of the initial xylose concentration. In comparison, the SA-1 XR/XDH strain consumed 30.38 ± 0.15 g of xylose, representing 89.6% of the initial xylose concentration. Additionally, at this time point, the

evolved and parental strains presented an OD_{600} of 17.7 ± 1.1 and 45.2 ± 2.1, respectively.

Finally, the evolved strain presented a higher production of glycerol (43%) and xylitol (61%) as by-products, while exhibiting lower growth when compared to the parental strain. At 72 h of fermentation, the evolved strain achieved 1.16 ± 0.05 g L^{-1} of xylitol, whereas the parental strain reached 0.45 ± 0.01 g L^{-1}. Glycerol and xylitol yield on xylose were 0.016 ± 0.001 g glycerol g $xylose^{-1}$ and 0.036 ± 0.002 g xylitol g $xylose^{-1}$ for the evolved strain, and 0.011 ± 0.001 g glycerol g $xylose^{-1}$ and 0.018 ± 0.001 g xylitol g $xylose^{-1}$ for the parental strain, respectively. Altogether, these results suggest that in hydrolysate fermentations with the evolved strain, xylose was consumed with a faster rate as compared to fermentation with the parental strain, while ethanol yield was kept virtually the same for both strains and xylose was directed towards metabolites that contributed to the maintenance of redox cofactor balance, such as xylitol and glycerol, in the former strain.

Conclusions

Laboratory adaptive evolution provided an improvement in SA-1 XR/XDH strain, mainly concerning the xylose. This dataset demonstrates the feasibility of this strategy. The evolved strain, DPY06, was able to consume xylose faster, presenting a specific xylose consuming rate 72% higher than the control cultivation, and showed an improvement in the volumetric ethanol productivity, 28% comparing DPY06 and SA-1 XR/XDH at 24 h of cultivation in YP media supplemented with glucose and xylose. The laboratory evolution was performed in long-term chemostats in defined medium under controlled conditions. Although we have verified that the evolved strain performed with faster rates than the parental strain at elevated sugar concentrations under anaerobic conditions, as well as in hemicellulosic hydrolysate-based medium, many other parameters relevant for industrial second-generation ethanol production remain to be systematically investigated.

Acknowledgement

We thank MSc. Gabriel C. de Gois e Cunha for helping with analytical methods, and Dr. Bruno L. V. da Costa for assisting with bioreactor operation. We are also grateful to Dr. Jeffrey M. Skerker and Prof. Adam P. Arkin for guidance on engineering yeast strain SA-1 XR/XDH.

Supplementary data

Supplementary data are available at *LAMBIO Journal* online.

Conflicts of interest

The authors declare no conflict of interest.

Funding

This research was funded by the Fundação de Apoio à Pesquisa do Estado de São Paulo (FAPESP) grants #2015/50612–8, #2018/17172–2, #2018/01759–4, and #2019/18075–3.

Author contributions

Thalita Peixoto Basso (Data curation [equal], Investigation [equal], Methodology [equal]), Dielle Pierotti Procópio (Data curation [equal], Formal analysis [equal], Investigation [equal], Methodology [equal], Supervision [equal], Validation [equal], Writing – original draft [equal]), Thais Helena Costa Petrin (Methodology [equal]), Thamiris Guerra Giacon (Methodology [equal]), Yong-Su Jin (Formal analysis [equal], Supervision [equal]), Thiago Olitta Basso (Conceptualization [equal], Formal analysis [equal], Project administration [equal], Resources [lead], Supervision [lead], Writing – review & editing [equal]), and Luiz Carlos Basso (Conceptualization [lead], Formal analysis [lead])

Data availability

The data underlying this article are available in the article and in its online supplementary material.

References

Basso LC, de Amorim HV, de Oliveira AJ *et al*. Yeast selection for fuel ethanol production in Brazil. *FEMS Yeast Res* 2008;**8**:1155–63. https://doi.org/10.1111/j.1567-1364.2008.00428.x

Basso TO, Dario MG, Tonso A *et al*. Insufficient uracil supply in fully aerobic chemostat cultures of *Saccharomyces cerevisiae* leads to respiro-fermentative metabolism and double nutrient-limitation. *Biotechnol Lett* 2010;**32**:973–7. https://doi.org/10.1007/s10529-010-0248-2

Brenelli LB, Figueiredo FL, Damasio A *et al*. An integrated approach to obtain xylo-oligosaccharides from sugarcane straw: from lab to pilot scale. *Bioresour Technol* 2020;**313**:123637. https://doi.org/10.1016/j.biortech.2020.123637

Brink DP, Borgström C, Persson VC *et al*. D-xylose sensing in *Saccharomyces cerevisiae*: insights from D-glucose signaling and native D-xylose utilizers. *IJMS* 2021;**22**:12410. https://doi.org/10.3390/ijms222212410.

Cola P, Procópio DP, Alves ATdC *et al*. Differential effects of major inhibitory compounds from sugarcane-based lignocellulosic hydrolysates on the physiology of yeast strains and lactic acid bacteria. *Biotechnol Lett* 2020;**42**:571–82. https://doi.org/10.1007/s10529-020-02803-6

Cunha JT, Soares PO, Romaní A *et al*. Xylose fermentation efficiency of industrial Saccharomyces cerevisiae yeast with separate or combined xylose reductase/xylitol dehydrogenase and xylose isomerase pathways. *Biotechnol Biofuels* 2019;**12**:1–14.

Cunha JT, Soares PO, Baptista SL *et al*. Engineered *Saccharomyces cerevisiae* for lignocellulosic valorization: a review and perspectives on bioethanol production. *Bioengineered* 2020;**11**:883–903. https://doi.org/101080/2165597920201801178

Della-Bianca BE, Gombert AK. Stress tolerance and growth physiology of yeast strains from the Brazilian fuel ethanol industry. *Antonie Van Leeuwenhoek* 2013;**104**:1083–95. https://doi.org/10.1007/s10482-013-0030-2

Dias Lopes D, Carlos RA, Ronald HE *et al*. Influence of genetic background of engineered xylose-fermenting industrial *Saccharomyces cerevisiae* strains for ethanol production from lignocellulosic hydrolysates. *J Ind Microbiol Biotechnol* 2017;**44**:1575–88. https://doi.org/10.1007/s10295-017-1979-z

Dos Santos LV, Carazzolle MF, Nagamatsu ST *et al*. Unraveling the genetic basis of xylose consumption in engineered *Saccharomyces cerevisiae* strains. *Sci Rep* 2016;**6**:38676. https://doi.org/10.1038/srep38676

Gietz RD, Woods RA. Transformation of yeast by lithium acetate/single-stranded carrier DNA/polyethylene glycol method. *Methods Enzymol* 2002;**350**:87–96. https://doi.org/10.1016/S0076-6879(02)50957-5

Jeong D, Oh EJ, Ko JK *et al*. Metabolic engineering considerations for the heterologous expression of xylose-catabolic pathways in *Saccharomyces cerevisiae*. *PLoS One* 2020;**15**:1–18. https://doi.org/10.1371/journal.pone.0236294

Kim SR, Ha SJ, Kong II *et al*. High expression of XYL2 coding for xylitol dehydrogenase is necessary for efficient xylose fermentation by engineered *Saccharomyces cerevisiae*. *Metab Eng* 2012;**14**:336–43. https://doi.org/10.1016/j.ymben.2012.04.001

Kim SR, Skerker JM, Kang W *et al*. Rational and evolutionary engineering approaches uncover a small set of genetic changes efficient for rapid xylose fermentation in *Saccharomyces cerevisiae*. *PLoS One* 2013;**8**:1–13.

Kuyper M, Winkler AA, Van Dijken JP *et al*. Minimal metabolic engineering of *Saccharomyces cerevisiae* for efficient anaerobic xylose fermentation: a proof of principle. *FEMS Yeast Res* 2004;**4**:655–64. https://doi.org/10.1016/j.femsyr.2004.01.003

Li H, Shen Y, Wu M *et al*. Engineering a wild-type diploid *Saccharomyces cerevisiae* strain for second-generation bioethanol production. *Bioresour Bioprocess* 2016;**3**:1–17. https://doi.org/10.1186/s40643-016-0126-4

Mavrommati M, Daskalaki A, Papanikolaou S *et al*. Adaptive laboratory evolution principles and applications in industrial biotechnology. *Biotechnol Adv* 2022;**54**:1–31. https://doi.org/10.1016/j.biotechadv.2021.107795

Osiro KO, Brink DP, Borgström C *et al*. Assessing the effect of D-xylose on the sugar signaling pathways of *Saccharomyces cerevisiae* in strains engineered for xylose transport and assimilation. *FEMS Yeast Res* 2018;**18**:96. https://doi.org/10.1093/femsyr/fox096

Procópio DP, Kendrick E, Goldbeck R *et al*. Xylo-oligosaccharide utilization by engineered *Saccharomyces cerevisiae* to produce ethanol. *Front Bioeng Biotechnol* 2022;**10**:1–21. https://doi.org/10.3389/fbioe.2022.825981

Qiu Y, Wu M, Bao H *et al*. Engineering of *Saccharomyces cerevisiae* for co-fermentation of glucose and xylose: current state and perspectives. *Eng Microbiol* 2023;**3**:100084. https://doi.org/10.1016/j.engmic.2023.100084

Romaní A, Pereira F, Johansson B *et al*. Metabolic engineering of *Saccharomyces cerevisiae* ethanol strains PE-2 and CAT-1 for efficient lignocellulosic fermentation. *Bioresour Technol* 2015;**179**:150–8. https://doi.org/10.1016/j.biortech.2014.12.020

Ryan OW, Skerker JM, Maurer MJ *et al*. Selection of chromosomal DNA libraries using a multiplex CRISPR system. *Elife* 2014;**3**:1–15. https://doi.org/10.7554/eLife.03703

Salusjärvi L, Kankainen M, Soliymani R *et al*. Regulation of xylose metabolism in recombinant *Saccharomyces cerevisiae*. *Microb Cell Fact* 2008;**7**:1–16. https://doi.org/10.1186/1475-2859-7-18

Sonderegger M, Sauer U. Evolutionary engineering of *Saccharomyces cerevisiae* for anaerobic growth on xylose. *Appl Environ Microbiol* 2003;**69**:1990–8. https://doi.org/10.1128/AEM.69.4.1990-1998.2003

Van Vleet JH, Jeffries TW. Yeast metabolic engineering for hemicellulosic ethanol production. *Curr Opin Biotechnol* 2009;**20**:300–6. https://doi.org/10.1016/j.copbio.2009.06.001

Verduyn C, Postma E, Scheffers WA *et al*. Effect of benzoic acid on metabolic fluxes in yeasts: a continuous-culture study on the regulation of respiration and alcoholic fermentation. *Yeast* 1992;**8**:501–17. https://doi.org/10.1002/yea.320080703

Wahlbom CF, Otero RRC, Zyl WHV *et al*. Molecular analysis of a *Saccharomyces cerevisiae* mutant with improved ability to utilize xylose shows enhanced expression of proteins involved in transport, initial xylose metabolism, and the pentose phosphate pathway. *Appl Environ Microbiol* 2003;**69**:740–6.

Received: December 15, 2022. **Revised:** May 31, 2023. **Accepted:** July 5, 2023